Article

Duplex Formation and the Onset of Helicity in Poly d(CG) Oligonucleotides in a Solvent-Free Environment

Jennifer Gidden, Alessandra Ferzoco, Erin Shammel Baker, and Michael T. Bowers

More About This Article

Additional resources and features associated with this article are available within the HTML version:

- Supporting Information
- Links to the 7 articles that cite this article, as of the time of this article download
- Access to high resolution figures
- Links to articles and content related to this article
- Copyright permission to reproduce figures and/or text from this article

View the Full Text HTML

Duplex Formation and the Onset of Helicity in Poly d(CG)$_n$ Oligonucleotides in a Solvent-Free Environment

Jennifer Gidden, Alessandra Ferzoco, Erin Shammel Baker, and Michael T. Bowers*

Contribution from the Department of Chemistry & Biochemistry, University of California, Santa Barbara, California 93106

Received June 16, 2004; E-mail: bowers@chem.ucsb.edu

Abstract: The gas-phase conformations of a series of cytosine/guanine DNA duplexes were examined by ion mobility and molecular dynamics methods. Deprotonated duplex ions were formed by electrospray ionization, and their collision cross sections measured in helium were compared to calculated cross sections of theoretical models generated by molecular dynamics. The 4-mer (dCGCG) and 6-mer (dCGCGCG) duplexes were found to have globular conformations. Globular and helical structures were observed for the 8-mer (dCGCGCGCG) duplex, with the globular form being the more favored conformer. For the 10-mer (dCGCGCGCGCG), 14-mer (dCGCGCGCGCGCGCG), and 18-mer (dCGCGCGCGCGCGCGCGCG) duplexes, only helical structures were observed in the ion mobility measurements. Theory predicts that the helical structures are less stable than the globular forms in the gas phase and should collapse into the globular form given enough time. However, molecular dynamics simulations at 300 K indicate the helical structures are stable in aqueous solution and will retain their conformations for a limited time in the gas phase. The presence of helical structures in the ion mobility experiments indicates that the duplexes retain "solution structures" in the gas phase on the millisecond time scale.

Introduction

In 1989, Fenn and co-workers demonstrated that gas-phase ions of large biological molecules could be generated and detected by electrospray ionization mass spectrometry (ESI-MS).[1] Two years later, Katta and Chait[2] and Ganem et al.[3] reported that specific noncovalent complexes could be transferred, intact, from solution to the gas phase using ESI-MS. Since that time, a number of review articles have been published that illustrate the usefulness of ESI-MS to study noncovalent complexes in the gas phase.[4–7] In fact, ESI has proven to be so invaluable in analyzing biological molecules in the gas phase that John Fenn was awarded a share of the 2002 Nobel Prize in Chemistry for its development.

One particular noncovalent complex that has attracted interest in ESI-MS studies is the DNA duplex. Held together by hydrogen bonding between specific bases on each strand (Watson–Crick pairs) and stabilized by base stacking within each strand, DNA duplexes are known to be quite robust.[8–10] Hydration is also believed to play a crucial role in stabilizing the duplex as it provides charge screening for the phosphate groups on the DNA backbone and changes to more apolar solvents have led to major disruptions in the double helical structure of the duplex.[11] Thus, the transfer of DNA duplexes from solution to the gas phase, where unscreened phosphates can repel each other and base stacking is presumably destabilized, should significantly reduce the chances for the survival of the duplexes.[11] However, DNA duplexes have been observed in mass spectra for over 10 years. In 1993, Light-Wahl et al. and Ganem et al. reported that 20-mer DNA duplexes[12] and 8-mer DNA duplexes[13] could be observed by ESI-MS. Since that time, DNA duplexes with as few as 1 base pair and as many as 500 base pairs have been observed by mass spectrometry.[14,15] Although many different DNA duplexes have been studied by ESI-MS, a prevailing question is whether the duplexes (or any noncovalent complex) retain any of their solution-phase structural features once the solvent is removed.

A number of mass spectrometry studies have shown that there may, indeed, be a certain level of conservation of the DNA structure in the gas phase. Dissociation kinetics of a series of 7-mer duplexes studied by blackbody infrared dissociation (BIRD) yielded higher activation energies for complementary duplexes as compared to noncomplementary ones, and a correlation was observed between these activation energies and

(1) Fenn, J. B.; Mann, M.; Meng, C. K.; Wong, S. F.; Whitehouse, C. M. *Science* **1989**, *246*, 64.
(2) Katta, V.; Chait, B. T. *J. Am. Chem. Soc.* **1991**, *113*, 8534.
(3) Ganem, B.; Li, Y.-T.; Henion, J. D. *J. Am. Chem. Soc.* **1991**, *113*, 6294.
(4) Hofstadler, S. A.; Griffey, R. H. *Chem. Rev.* **2001**, *101*, 377.
(5) Loo, J. A. *Mass Spectrom. Rev.* **1997**, *16*, 1.
(6) Veenstra, T. D. *Biochem. Biophys. Res. Commun.* **1999**, *257*, 1.
(7) Smith, R. D.; Light-Wahl, K. J. *Biol. Mass Spectrom.* **1993**, *22*, 493.
(8) Watson, J. D.; Crick, F. H. *Nature* **1953**, *171*, 1303.
(9) Blackburn, G. M.; Gait, M. J. *Nucleic Acids in Chemistry and Biology*; IRL Press: Oxford, 1990.
(10) Bloomfield, V. A.; Crothers, D. M.; Tinoco, I. *Nucleic Acids. Structure, Properties, and Function*; University Science Books: Sausalito, 2000.

(11) Sinden, R. R. *DNA Structure and Function*; Academic Press: San Diego, CA, 1994.
(12) Light-Wahl, K. J.; Springer, D. L.; Winger, B. E.; Edmonds, C. G.; Camp, D. G.; Thrall, B. D.; Smith, R. D. *J. Am. Chem. Soc.* **1993**, *115*, 803.
(13) Ganem, B.; Li, Y.-T.; Henion, J. D. *Tetrahedron Lett.* **1993**, *34*, 1445.
(14) Baker, E. S.; Gidden, J.; Ferzoco, A.; Bowers, M. T. *Phys. Chem. Chem. Phys.* **2004**, *6*, 2786.
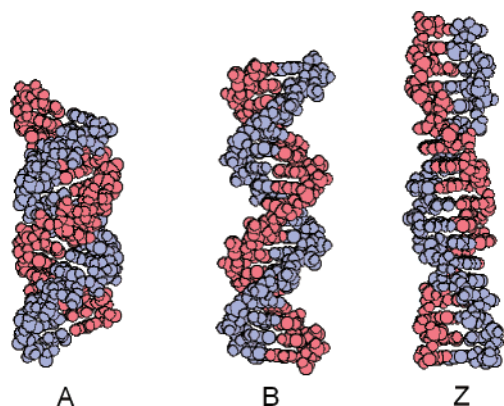(15) Muddiman, D. C.; Null, A. P.; Hannis, J. C. *Rapid Commun. Mass Spectrom.* **1999**, *13*, 1201.

Figure 1. Space-filling models of the three most common helices observed for DNA duplexes in the condensed phase. (a) A-form (found at low humidity), (b) B-form (found at high humidity), and (c) Z-form (found for alternating purine−pyrimidine sequences with high salt concentrations). One strand is shown in blue, and the other is shown in red.

the enthalpies of dimerization in solution.[16] These results suggested that Watson−Crick pairing was being retained in the gas phase. Collision-induced dissociation (CID) studies on 12-mer and 16-mer duplexes yielded fragmentation results that correlated with thermal denaturation curves[17,18] and enthalpies of dissociation[19] in solution, suggesting a conservation of DNA structure in the gas phase. Other CID studies have shown that gas-phase cleavage of duplexes is directed toward mismatched base pairs.[20] H/D exchange studies on DNA oligonucleotides showed a decrease in the rate of exchange for duplexes as compared to single strands, indicating the duplexes may be protected by internal Watson−Crick pairing.[21]

Although these studies indicate that DNA duplexes conserve a certain portion of their solution-phase character in the gas phase, their overall conformation remains a major question. In solution, the most common conformations of the DNA duplex are the double helices shown in Figure 1. Under normal physiological conditions, the duplex is usually in a B-DNA form, which is a right-handed double helix.[22,23] A-DNA is another right-handed double helix, shorter and wider than B-DNA, that has been observed under low humidity conditions.[24] Z-DNA is a left-handed double helix, more elongated and slender than B-DNA, that has been primarily observed in alternating cytosine/guanine-rich sequences under high salt concentrations.[25] However, there has been no direct experimental data indicating whether these helices exist in the gas phase.

There have been theoretical studies that have addressed this issue. Rueda et al., for example, performed lengthy 300 K molecular dynamics simulations on a 12-mer and 16-mer duplex,

containing the sequence dCGCGAATTCGCG, in water and in vacuo.[26] They reported that an elongated, distorted double-helix structure could exist once the solvent was removed for up to 250 ns. This gas-phase helix contained many of the same structural features found in water such as hydrogen bonding and base stacking (although these features were better preserved in the G·C regions than the A·T regions). Schnier et al. performed short MD simulations on dA$_7$·dT$_7$, dA$_7$·dA$_7$, and dT$_7$·dT$_7$ duplexes in a solvent-free environment.[16] They discovered that the dA$_7$·dT$_7$ duplex retained all 7 A·T pairs after 100 ps (and 6 of 7 pairs after 400 ps), although the helix partially collapsed. The other two duplexes (dA$_7$·dA$_7$ and dT$_7$·dT$_7$), on the other hand, collapsed into ball-like structures after 40 ps of dynamics.

In this paper, we address this issue by reporting on the gas-phase conformations of a series of duplexes containing cytosine and guanine [d(CG)$_n$·d(CG)$_n$, $n = 2-9$] using ion mobility and molecular modeling methods. [d(CG)$_n$·d(CG)$_n$] ions were sprayed from solution using ESI, and their collision cross sections in helium were measured using ion mobility-based methods.[27,28] Structural information about the ions was obtained by comparing the experimental cross sections to calculated values of low-energy structures obtained from theoretical modeling.

Experimental Section

Ion Mobility Experiments. Poly d(CG)$_n$ oligonucleotides ($n = 2-9$) were purchased from Sigma-Genosys (The Woodlands, TX) and were used without further purification. The oligonucleotides were resuspended at a concentration of 300 μM in a 20 mM NH$_4$OAc/H$_2$O solution (pH 7.0). They were annealed at 95 °C for 5 min, slowly cooled to room temperature (or below their T_m), and stored at 10 °C, except for the 4-mer and 6-mer which were stored at 0 °C. The duplex solutions were then diluted to 75 μM and sprayed in a 98:2 (v/v) NH$_4$OAC/NH$_4$OH solution or a 49:49:2 H$_2$O/MeOH/NH$_4$OH solution.

The instrument used for the ion mobility measurements has previously been described in detail,[29] so only a brief description will be given here. Ions are generated by nanoelectrospray ionization and injected into an ion funnel via a 3-in. long capillary. The voltage applied to the needle is typically between 1 and 2 kV with respect to the capillary. The ion funnel essentially acts as an ion guide, compressing the stream of ions exiting the capillary and directing them toward the drift cell. The funnel is also used as an ion trap, allowing conversion of the continuous ion beam from the ESI source into a short ion pulse for the mobility measurements without diminishing the total ion current. After injection into a 4.5 cm long drift cell, the ions are quickly thermalized by collisions with ~5 Torr of helium gas and drift through the cell under the influence of a weak, uniform electric field (10−25 V/cm). Ions exiting the cell are mass analyzed with a quadrupole mass filter and detected as a function of time, yielding an arrival time distribution (ATD) collected on a multichannel scalar.

To quantitatively measure the ion mobility and collision cross section, the following procedure is utilized.[30−32] A pulse of ions is injected at

(16) Schnier, P. D.; Klassen, J. S.; Strittmatter, E. F.; Williams, E. R. *J. Am. Chem. Soc.* **1998**, *120*, 9605.
(17) Gabelica, V.; DePauw, E. *J. Mass Spectrom.* **2001**, *36*, 397.
(18) Gabelica, V.; Rosu, F.; Houssier, C.; DePauw, E. *Rapid. Commun. Mass Spectrom.* **2000**, *14*, 464.
(19) Gabelica, V.; DePauw, E. *Int. J. Mass Spectrom.* **2002**, *219*, 151.
(20) Griffey, R. H.; Greig, M. J.; An, H.; Sasmor, H.; Manalili, S. *J. Am. Chem. Soc.* **1999**, *121*, 474.
(21) Hofstadler, S. A.; Sannes-Lowery, K. A.; Griffey, R. H. *J. Mass Spectrom.* **2000**, *35*, 62.
(22) Langridge, R.; Wilson, H. R.; Hooper, C. W.; Wilkins, M. H. F.; Hamilton, L. D. *J. Mol. Biol.* **1960**, *2*, 19.
(23) Langridge, R.; Marvin, D. A.; Seeds, W. E.; Wilson, H. R.; Hamilton, L. D. *J. Mol. Biol.* **1960**, *2*, 38.
(24) Fuller, W.; Wilkins, M. H. F.; Wilson, H. R.; Hamilton, L. D.; Arnott, S. *J. Mol. Biol.* **1965**, *12*, 60.
(25) Wang, A. H. J.; Quigley, G. J.; Kolpak, F. J.; Crawford, J. L.; vanBoom, J. H.; van derMarel, G.; Rich, A. *Nature* **1979**, *282*, 680.

(26) Rueda, M.; Kalko, S. G.; Lique, F. J.; Orozco, M. *J. Am. Chem. Soc.* **2003**, *125*, 8007.
(27) Bowers, M. T.; Kemper, P. R.; vonHelden, G.; vanKoppen, P. A. M. *Science* **1993**, *260*, 1446.
(28) For reviews, see: Clemmer, D. E.; Jarrold, M. F. *J. Mass Spectrom.* **1997**, *32*, 577. Wyttenbach, T.; Bowers, M. T. *Top. Curr. Chem.* **2003**, *225*, 207.
(29) Wyttenbach, T.; Kemper, P. R.; Bowers, M. T. *Int. J. Mass Spectrom.* **2001**, *212*, 13.
(30) Kemper, P. R.; Bowers, M. T. *J. Am. Soc. Mass Spectrom.* **1990**, *1*, 197.
(31) vonHelden, G.; Hsu, M.-T.; Gotts, N.; Bowers, M. T. *J. Am. Chem. Soc.* **1993**, *115*, 8182.
(32) Gidden, J.; Kemper, P. R.; Shammel, E.; Fee, D. P.; Anderson, S. E.; Bowers, M. T. *Int. J. Mass Spectrom.* **2003**, *222*, 63.

low energy into the mobility cell. A weak, homogeneous electric field, E, is applied across the cell, causing the ion packet to drift toward an exit aperture. Collisions with the helium buffer gas bath broaden the ion packet width and serve to bring a balance between the force imposed by the electric field and the frictional drag force. As a consequence, the ions drift at constant velocity, v_D, proportional to the applied field E:

$$v_D = KE \tag{1}$$

The proportionality constant, K, is termed the mobility. To obtain values independent of temperature T and pressure p, the reduced mobility K_o is usually determined:

$$K_o = \left(K \frac{p}{760} \frac{273.16}{T} \right) \tag{2}$$

Kinetic theory has been applied[33] to this system, resulting in an expression of K_o as a function of the collision system parameters.

$$K_o = \frac{3q}{16N} \left(\frac{2\pi}{\mu k_b T} \right)^{1/2} \frac{1}{\Omega^{(1,1)}} \tag{3}$$

where q is the ion charge, N is the buffer gas density, m is the reduced mass of the collision partners, k_b is Boltzmann's constant, and $\Omega^{(1,1)}$ is the collision integral. For hard sphere collisions, $\Omega^{(1,1)}$ is identical to the collision cross section. Using eqs 1–3, it is straightforward to obtain an expression for the arrival time t_A in terms of the instrument and molecular parameters:

$$t_A = \frac{l^2}{K_o} \frac{273.16}{760T} \frac{p}{V} + t_o \tag{4}$$

where l is the drift cell length, V is the voltage across the cell, and t_o is the time the ions spend outside the drift cell before detection. Hence, a simple plot of p/V versus t_A yields K_o from the slope and thus the cross section using eq 3. In a typical experiment, the pressure is held constant, while four or five different drift voltages are applied. The resultant plots are always very linear with correlation values near 0.9999. Multiple measurements are made on each system with reproducibility better than 1%. These small variations are probably due to small pressure fluctuations during the measurements.

In all experiments reported here, the ATDs were measure over a wide range of injection voltages (10–100 eV). In all cases, similar ATDs were obtained, indicating neither isomerization nor dissociation was induced during the ion mobility process.

Calculations. Structural information about the ions is obtained by comparing the experimental cross sections determined from the ATDs to calculated values of theoretical models. Candidate structures of the d(CG)$_n$·d(CG)$_n$ duplex ions were generated using the AMBER 7.0[34] set of programs with the parm99 force field.[35] Canonical A- and B-form starting geometries were created using the NUCGEN utility within AMBER, and Z-forms were generated using Hyperchem.[36] A series of simulated annealing/energy minimization cycles were then used to generate hundreds of low-energy gas-phase structures of each duplex. This process has been successful in generating low-energy structures that match experimental data for numerous biological and synthetic

polymers[37–41] and is described as follows. The initial structures are energy minimized, annealed at 700 K for 30 ps (to allow the structure to overcome low-lying barriers and change shape), exponentially cooled to 50 K over a variable time step, and energy minimized again. The final structure is saved and used as the starting structure for another annealing/minimization cycle. The process is continued until 300–400 low-energy structures are generated.

For ions with less than 200 atoms, the angle-averaged collision cross section of each structure is calculated using a temperature-dependent projection model.[42,43] For larger ions, collision cross sections of each structure are calculated using hard-sphere scattering and trajectory models developed by the Jarrold group.[44,45] The average cross section of the lowest 5–15 kcal/mol structures (which typically have only minor structural differences) are then compared to experiment. In some cases, families of conformers can be identified in the theoretical modeling, and so the average cross section of each family is compared to experiment.[38–41]

ESI studies of DNA typically yield negative ions because of the ease at which the phosphate groups can be deprotonated. The overall charge state of the duplex can be readily identified from the mass spectra, but the exact locations of the deprotonation sites, needed for the modeling, are not known. However, two sets of data exist that aid in the assignment of charge sites. First, CID studies on DNA duplexes, in which the main fragmentation pathway is the dissociation of the duplex into its two individual strands, indicate that the overall charge tends to be more or less evenly distributed among the two strands (i.e., AB^{7-} fragments into A^{4-} and B^{3-}).[16–19] This particular charge distribution may be the result of a number of unrelated things but certainly provides a starting point for assigning charge sites. Second, ion mobility measurements on $[T_{10} - nH]^{n-}$ single-stranded oligonucleotides have shown that the best agreement between experimental and theoretical cross sections occurs when the deprotonation sites are dispersed along the phosphate backbone rather than placed on adjacent phosphates.[46] Thus, the deprotonation sites on the d(CG)$_n$·d(CG)$_n$ duplex ions were divided among the two strands and dispersed along each strand, with at least two neutral phosphate groups between every deprotonated group.

The 8-mer duplex was also modeled in solution by placing the initial B-DNA structure in a water box. The box contained ~1200 water molecules that were parametrized with the TIP3P model.[47] Equilibration of the system was performed as follows. An initial minimization of 1000 steps using steepest descent methods with 500 kcal/mol·Å^2 positional restraints on the DNA duplex was followed by 25 ps of molecular dynamics (with 1 fs time steps) at 300 K and constant pressure. This was followed by another 1000-step steepest descent minimization with 25 kcal/mol·Å^2 position restraints and 3 ps of molecular dynamics at 300 K. A series of 600-step minimizations were then used in which the positional restraints were reduced by 5 kcal/mol·Å^2 each time. The final structures (with no restraints) were then heated from 100 to 300 K over 2 ps. The production run dynamics were run for 10 ns at 300 K, and structures were saved every 500 ps.

(33) Mason, E. A.; McDaniel, E. W. *Transport Properties of Ions in Gases*; Wiley: New York, 1988.
(34) Case, D. A.; Pearlman, D. A.; Caldwell, J. W.; Cheatham, T. E., III; Wang, J.; Ross, W. S.; Simmerling, C. L.; Darden, T. A.; Merz, K. M.; Stanton, R. V.; Cheng, A. L.; Vincent, J. J.; Crowley, M.; Tsui, V.; Gohlke, H.; Radmer, R. J.; Duan, Y.; Pitera, J.; Massova, I.; Seibel, G. L.; Singh, U. C.; Weiner, P. K.; Kollman, P. A. *AMBER 7*; University of California, San Francisco, 2002.
(35) Cheatham, T. E.; Cieplak, P.; Kollman, P. A. *J. Biomol. Struct. Dyn.* **1999**, *16*, 8458.
(36) Hyperchem 7.0, Hypercube Inc., 2002.

(37) Wyttenbach, T.; von Helden, G.; Bowers, M. T. *J. Am. Chem. Soc.* **1996**, *118*, 8355.
(38) Gidden, J.; Wyttenbach, T.; Batka, J. J.; Weis, P.; Jackson, A. T.; Scrivens, J. H.; Bowers, M. T. *J. Am. Soc. Mass Spectrom.* **1999**, *10*, 883.
(39) Gidden, J.; Bowers, M. T. *Eur. Phys. J. D* **2002**, *20*, 409.
(40) Baker, E. S.; Gidden, J.; Fee, D. P.; Kemper, P. R.; Anderson, S. E.; Bowers, M. T. *Int. J. Mass Spectrom.* **2003**, *227*, 205.
(41) Gidden, J.; Bowers, M. T. *J. Am. Soc. Mass Spectrom.* **2003**, *14*, 161.
(42) Wyttenbach, T.; vonHelden, G.; Batka, J. J.; Carlat, D.; Bowers, M. T. *J. Am. Soc. Mass Spectrom.* **1997**, *8*, 275.
(43) Wyttenbach, T.; Witt, M.; Bowers, M. T. *J. Am. Chem. Soc.* **2000**, *122*, 3458.
(44) Mesleh, M. F.; Hunter, J. M.; Shvartsburg, A. A.; Schwartz, G. C.; Jarrold, M. F. *J. Phys. Chem.* **1996**, *100*, 16082.
(45) Shvartsburg, A. A.; Jarrold, M. F. *Chem. Phys. Lett.* **1996**, *261*, 86.
(46) Hoaglund, C. S.; Liu, Y.; Ellington, A. D.; Pagel, M.; Clemmer, D. E. *J. Am. Chem. Soc.* **1997**, *119*, 9051.
(47) Jorgensen, W. L.; Chandrasekhar, J.; Madura, J. D.; Impey, R. W.; Klein, M. L. *J. Chem. Phys.* **1983**, *79*, 926.
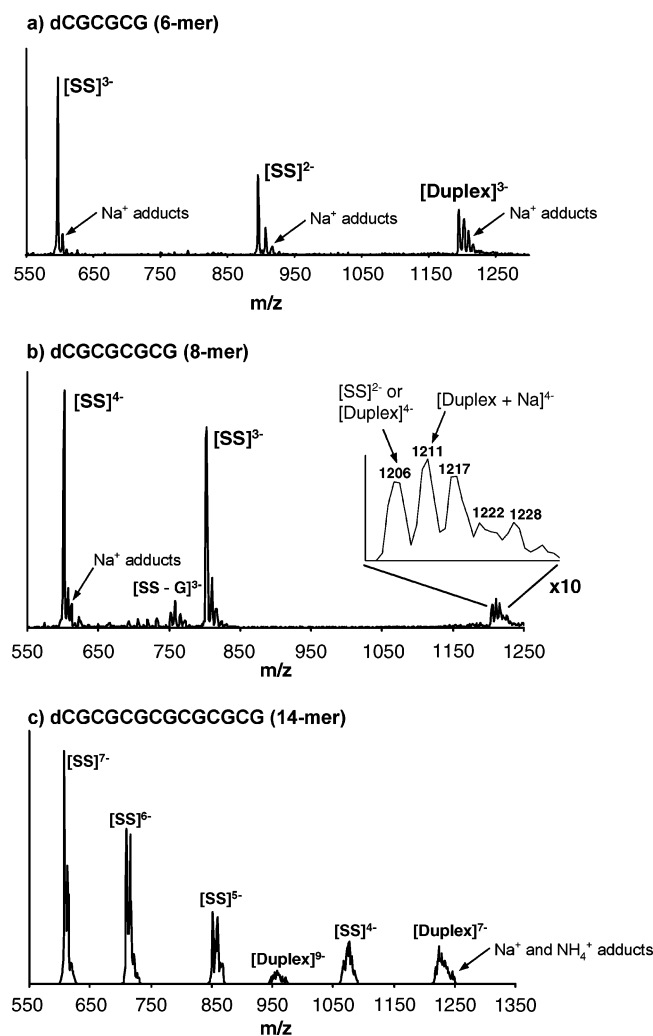
Figure 2. Electrospray ionization mass spectra of (a) dCGCGCG, (b) dCGCGCGCG, and (c) dCGCGCGCGCGCGCG. The spectra shown in (a) and (b) were obtained using a $H_2O/CH_3OH/NH_4OH$ spray solution, and the spectrum shown in (c) was obtained using an NH_4OAc/NH_4OH spray solution. The inset in (b) shows the sodium splitting for the −4 charge state of the 8-mer duplex. The abbreviation SS stands for single strand.

Results

Mass Spectra. Figure 2 shows ESI mass spectra of the poly d(CG) 6-mer, 8-mer, and 14-mer oligonucleotides. Deprotonated single-strand and duplex ions are present in the mass spectra of each oligonucleotide, but Na^+ and NH_4^+ adducts are observed as well. The spectra shown for the 6-mer and 8-mer were obtained using a $H_2O/CH_3OH/NH_4OH$ spray solution, but the spectrum shown for the 14-mer was obtained using the NHOAc/NH_4OH spray solution (which likely accounts for the increased abundance of NH_4^+ adducts). If the $H_2O/CH_3OH/NH_4OH$ solution is used to spray the 14-mer ions, the only significant differences in the mass spectra are the absences of the −9 charge state duplex and the NH_4^+ adducts. The duplex peaks are significantly smaller than the single strands (although they have enough intensity to perform ion mobility measurements). However, the focus of this study is on the ion mobility measurements, and so the mass spectra are mainly used to verify that duplexes have been formed and to identify the charge state of the ion.

To determine whether duplexes are actually formed in solution, circular dichroism spectra were obtained for the poly
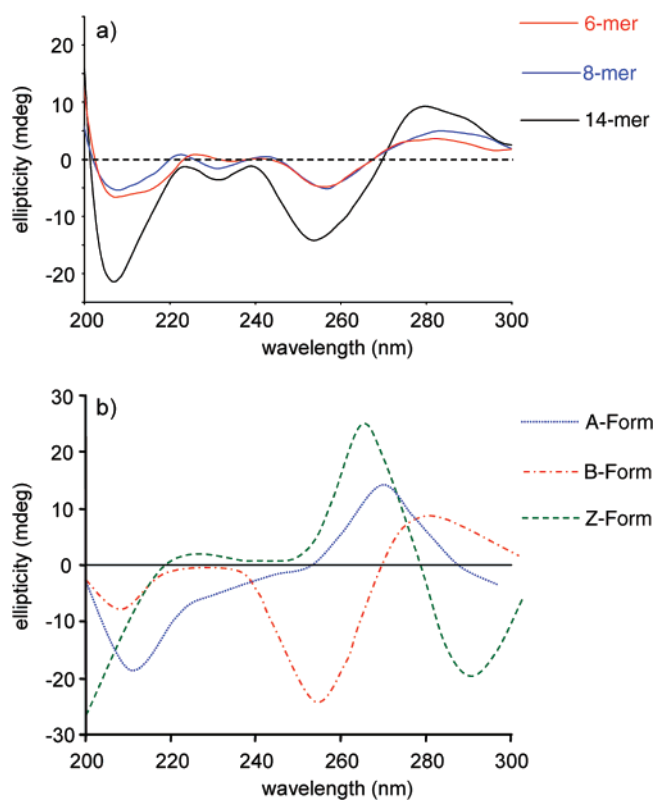

Figure 3. (a) CD spectra of the poly d(CG) 6-mer (red), 8-mer (blue), and 14-mer (black) in 50:50 H_2O/CH_3OH. (b) Expected CD spectra for A- (blue), B- (red), and Z-DNA (green) duplexes (see text).

d(CG) 6-mer, 8-mer, and 14-mer in a 50:50 H_2O/CH_3OH solution. The spectra were measured on an Olis RSM 1000 spectrometer using a 0.1 cm path length quartz cell and are shown in Figure 3a. CD spectra characteristic of A-, B-, and Z-DNA[48−51] are shown in Figure 3b. The spectra show a strong negative band near 255 nm and a positive band near 280 nm, which is characteristic of a B-DNA duplex (A-DNA and Z-DNA duplexes should yield spectra with a large maximum near 260−270 nm). The bands become more intense as the length of the oligonucleotide increases, which is expected as longer oligos should more easily form duplexes and single strands most likely still exist for the 6-mer and 8-mer oligos.

Because the poly d(CG) strands are self-complementary, care must be taken in assigning the peaks in the mass spectra. Duplexes with odd charge states can be unambiguously identified, but duplexes with even charge states have the same m/z value as single strands with half the number of charges. However, duplexes with even charge states can be identified by examining the difference in the m/z values of the Na^+ adducts associated with the duplex. Such a multiplet is shown for the 8-mer (with a −4 duplex) in the inset of Figure 2. In this 8-mer mass spectrum, the peak at m/z 1206 can be assigned to the deprotonated duplex with a −4 charge state or a single strand with a −2 charge state. However, each Na^+ added to the −2 single strand should yield a difference in m/z of 11. A −4 charge state duplex should yield a sodium splitting of m/z 5.5 for each

(48) Riazance, J. H.; Baase, W. A.; Johnson, W. C., Jr.; Hall, K.; Cruz, P.; Tinoco, I., Jr. *Nucleic Acids Res.* **1985**, *13*, 4983.
(49) Segersnolten, G. M. J.; Sijtsema, N. M.; Otto, C. *Biochemistry* **1997**, *36*, 13241.
(50) Poehl, F. M.; Jovin, T. M. *J. Mol. Biol.* **1972**, *67*, 375.
(51) Trantirek, L.; Stefl, R.; Vorlickova, M.; Koca, J.; Sklenar, V.; Kypr, J. I. *Mol. Biol.* **2000**, *297*, 907.

Na$^+$ added. Thus, the peak at m/z 1211 must be a sodiated duplex ion and is assigned as [duplex + Na − 5H].$^{4−}$ As will be shown in the ion mobility results, it is important to be able to unequivocally assign the duplexes in the mass spectra.

Ion Mobility. Arrival time distributions for the poly d(CG) duplexes, measured at 300 K, are shown in Figure 4. Spectra are shown for the 4-mer to the 18-mer. The ATD for the 8-mer is the sodiated adduct (m/z 1211) because it can be positively identified as a duplex on the basis of its m/z value and interference from single strands will not appear in the spectra. ATDs for the −9 charge state of the 14mer duplex and the −11 charge state of the 18mer duplex are similar to those obtained for the −7 and −9 charge states shown in Figure 4.

Single peaks are present in all of the ATDs, indicating that only one family of conformers is present, except for the 8-mer. In the latter case, two peaks are present in the ATD that are separated by 75 μs (corresponding to a difference in cross section of 130 Å^2). The ions are mass filtered after the drift cell, so the two peaks must be significantly different conformations of the duplex. The collision cross sections of each duplex, obtained from a series of ATDs with different voltages applied across the cell,[30−32] are listed in Table 1.

Discussion

4-mer and 6-mer Duplexes. Examples of the lowest energy structures of the 4-mer and 6-mer duplexes are shown in Figure 5. The duplexes were initially placed in a canonical A-, B-, and Z-DNA geometry, but they both immediately collapsed into more globular structures during the simulated annealing procedure. This is not a surprising result as neither duplex is long enough to constitute a full turn in a helix and the globular forms are significantly more stable (>100 kcal/mol) than the initial helical starting structures.

The 4-mer duplex most likely does not exist as a helix in solution because its T_m is 9 °C, but the lowest energy structure does have some residual interactions between bases in each strand. However, none of them are in a Watson−Crick arrangement. The Na$^+$ ion binds to a deprotonated phosphate[52] but also binds to carbonyl oxygens on the bases.[14] If two adjacent phosphate groups are deprotonated, the Na$^+$ ion will bridge both sites (as well as bind to a base). In the 6-mer duplex, two Watson−Crick pairs remain intact near each end of the duplex, but the two strands are very much intertwined, and the duplex has lost any sense of helicity.

The average cross sections of the lowest 5−10 kcal/mol globular structures of each duplex are compared to experimental values in Table 1. In each case, experiment and theory agree within 2%. Also listed in Table 1 are the calculated cross sections of the initial A-, B-, and Z-helical structures. The cross sections of the helices are ~15% larger than experimental values, well outside acceptable limits (±2%). Thus, these small duplexes can definitely be assigned to globular structures in the gas phase.

8-mer Duplex. Assignment of the 8-mer duplex structure is more complex because two peaks are present in the ATD (indicating two different conformers exist). The lowest energy structures of the 8-mer [duplex + Na − 5H]$^{4−}$ are globular, although 2−3 Watson−Crick pairs remain intact. This globular structure is shown in Figure 6a. As in the 4-mer duplex, the

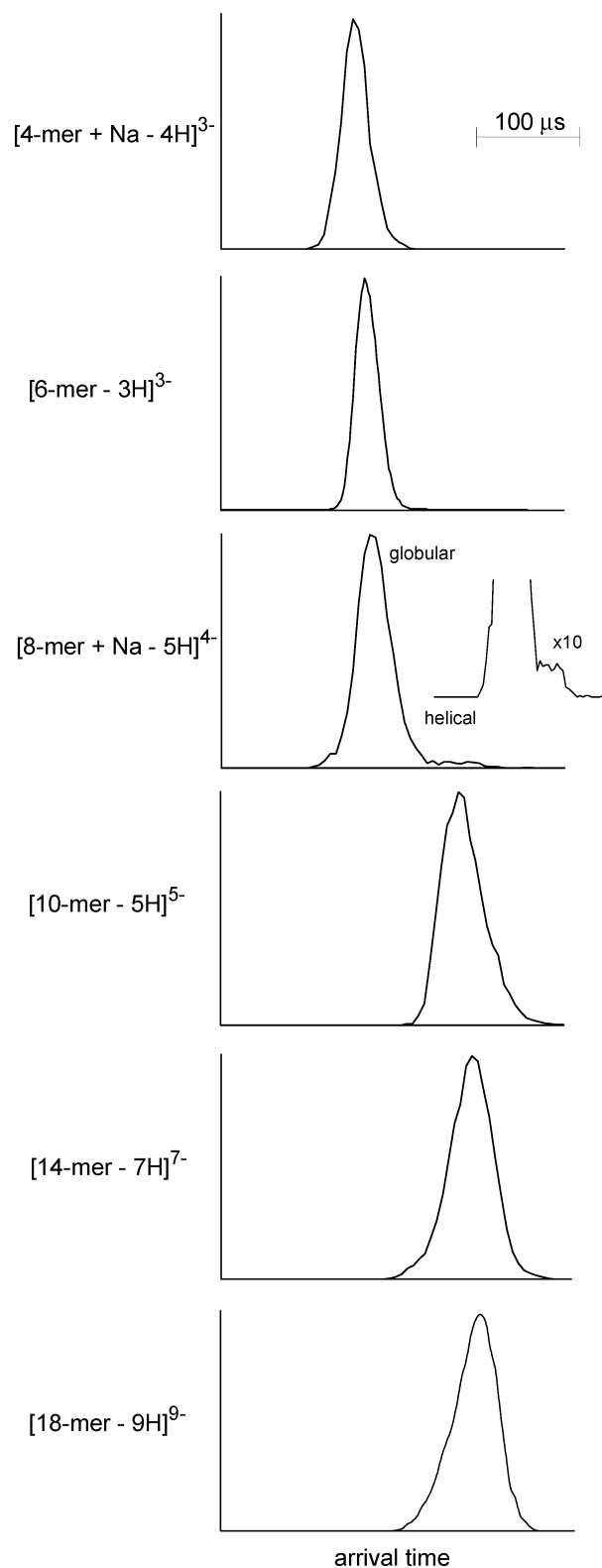(52) Favre, A.; Gonnet, F.; Tabet, J. C. *Int. J. Mass Spectrom.* **1999**, *191*, 303.

Figure 4. Arrival time distributions (ATDs) of the poly d(CG)$_n$ duplexes. In each instance, care was taken to ensure pure duplex peaks in the mass spectra were used for the ATDs (see text). Two peaks appear in the ATD of the 8-mer duplex, indicating two different conformations are present. Any small asymmetries in the remaining ATDs are due to noise and are not reproducible. Collision cross sections of the ions can be extracted from the ATDs and are listed in Table 1.

Na$^+$ ion binds primarily to the deprotonated phosphates but also binds to carbonyl oxygens on the bases. The average collision

Table 1. Experimental and Theoretical Collision Cross Sections (Å²) of the d(CG)n Duplexes

		theory[b]			
duplex	expt[a]	globular	A-helix	B-helix	Z-helix
[4mer + Na − 4H]³⁻	352	350	407	392	405
[6mer − 3H]³⁻	430	440	533	515	502
[8mer + Na − 5H]⁴⁻	536, 667	541	671	643	654
[10mer − 5H]⁵⁻	718	640	734	783	763
[14mer − 7H]⁷⁻	1006				
[14mer − 9H]⁹⁻	1013	850	1016	1034	1035
[14mer + NH₄ − 8H]⁷⁻	1011				
[18mer − 9H]⁹⁻	1268				
[18mer − 11H]¹¹⁻	1272	991	1254	1221	1205
[18mer + NH₄ − 10H]⁹⁻	1265				

[a] 1% reproducibility error. [b] Globular cross sections are averages of the lowest 5−10 kcal/mol structures; cross sections of the helices are of the starting helices for the 4-mer and 6-mer and are determined from 300 K dynamics simulations for the 8-mer to 18-mer (see text); ≤2% standard deviation.
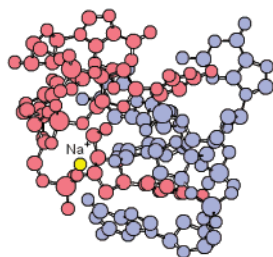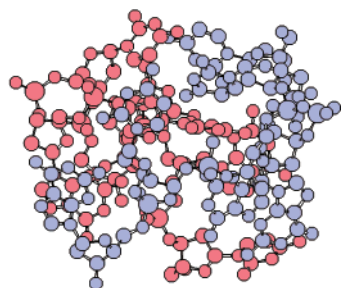
Figure 5. Lowest energy structures for the (a) 4-mer duplex with the addition of 1 Na⁺ ion and (b) 6-mer duplex. One strand is shown in red, and the other strand is shown in blue.

cross section of the globular structure agrees very well with the experimental cross section obtained from the fastest-time peak in the ATD (see Table 1). However, none of the 400 structures generated in the simulated annealing process have cross sections that match the experimental value derived from the longest-time peak in the ATD (667 Å²).

Structural studies on DNA in solution have shown that the double helix is quite stable when sufficiently hydrated, even for small duplexes.[9−11] This appears to be true for these poly d(CG) duplexes as well because the 8-mer duplex, when placed in a water box, retained its B-form helix throughout 10 ns of 300 K molecular dynamics simulations. However, extended molecular dynamics simulations (up to 250 ns) on complementary 12-mer and 16-mer duplexes in solution and the gas phase[26] have shown that the double helix is partially conserved in the gas phase for a limited time once the water box is removed. Therefore, the question arises: is the longest-time peak in the
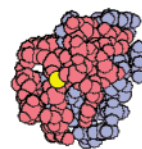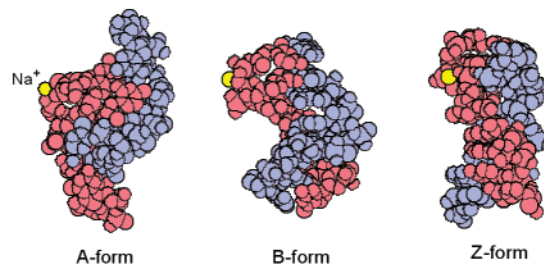
Figure 6. Space-filling models of the 8-mer [duplex + Na − 5H]⁴⁻ ion. (a) Lowest energy globular structures generated by the 700 K simulated annealing procedure. (b) Final structures after 2 ns of 300 K dynamics starting with canonical A-, B-, and Z-helices. One strand is illustrated in blue, and the other is in red.

8-mer ATD a helical structure that has retained its shape (to some extent) from solution?

To test this theory, the A-, B-, and Z-helix of the 8-mer duplex were investigated using 300 K molecular dynamics simulations (instead of the 700 K simulated annealing cycle). The dynamics were run for 2 ns, and every 5 ps the structure was saved and its cross section was calculated.[38] Plots of cross section versus time are shown in Figure 7. For the A- and B-helix, the cross sections decrease rapidly over the first 250 ps, but the helices appear to eventually find an "equilibrium" type structure, as the cross section remains relatively constant for the remainder of the simulation. The cross section of the B-helix decreases more rapidly than that of the A-helix and eventually yields a structure that has a smaller cross section than the A-helix. The cross section of the Z-helix decreases somewhat over the first 50 ps, but it quickly finds its "equilibrium" structure, which is very similar to the starting Z-helix.

The final structures of the A-, B-, and Z-forms, saved at the end of the dynamics runs, are shown in Figure 6b. The average cross section of the final 50−75 structures of each form are listed in Table 1. In each case, the Na⁺ ion stays near its initial position proximate to a deprotonated phosphate. Unlike in the globular form, where Na⁺ also binds to a base, the Na⁺ ion remains on the outside of the helix and does not bind to any of the bases. Molecular dynamics simulations on the deprotonated 8-mer duplex without Na⁺ yielded structures similar to those shown in Figure 6b.

In the A- and B-forms, 7 of the 8 Watson−Crick pairs remain intact, with the broken pair located ∼3 base-pairs from the end. In the Z-form, all 8 Watson−Crick pairs remain intact, and the final structure is similar to the initial Z-helix. Although the C and G bases are still paired, the final "gas-phase" helices bend and twist differently than their initial "condensed-phase" counterparts. Thus, helical parameters such as helix pitch, base tilt, and roll are not strictly defined A-, B-, or Z-parameters (although the sugar puckers and base orientations (syn vs anti) do remain the same). In any case, the cross sections of the
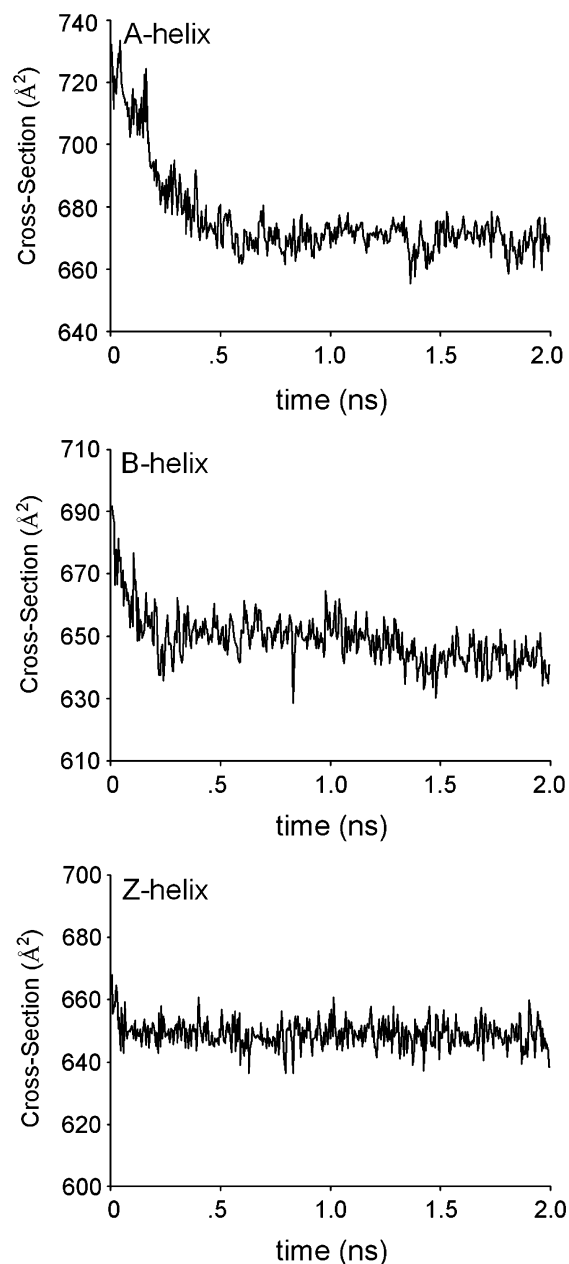
Figure 7. Plots of cross section versus dynamics time for the 8-mer [duplex + Na − 5H]$^{4-}$ ion. The initial geometry of the helix was the canonical (a) A-form, (b) B-form, and (c) Z-form. The dynamics simulations were run at 300 K for 2 ns. Every 5 ps, the structure was saved and its cross section was calculated.

Figure 8. Space-filling models of the 10-mer [duplex − 5H]$^{5-}$ ion. (a) Lowest energy globular structure generated by the 700 K simulated annealing procedure. (b) Final structures after 5 ns of 300 K dynamics when starting with A-, B-, and Z-helices. One strand is blue, and the other is red.

helices shown in Figure 6b agree well with the experimental value extracted from the longer-time peak in the ATD as shown in Table 1. The cross section of the A-form (671 Å^2) matches best with experiment, but the cross section of the Z-form (654 Å^2) is within 2% of experiment. The cross section of the B-form (643 Å^2) is ~3.5% smaller than experiment, due to the bend in the middle of the helix that occurs during the dynamics.

The helical structures shown in Figure 6b are >100 kcal/mol higher in energy than the globular form. Yet, the 8-mer duplex ATDs clearly show that helical structures are present in the gas phase. Because the globular form is not likely to isomerize into a helical structure in the gas phase, the ATD results indicate that at least some fraction of the 8-mer must have been helical in solution and a certain portion was
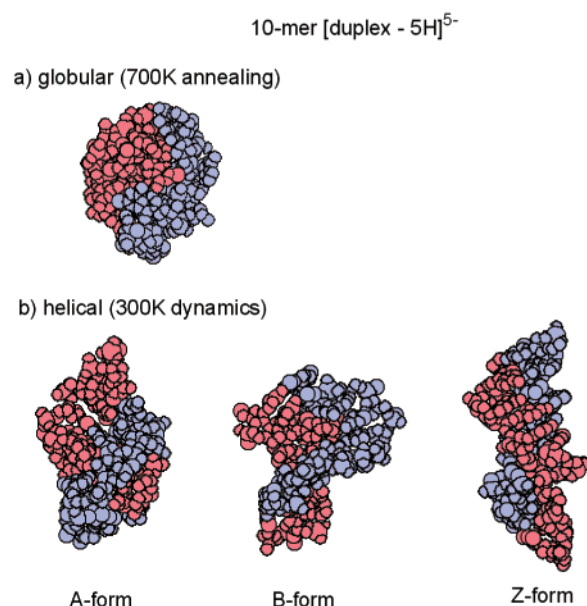
transferred intact into the gas phase. Once free of the solvent, the 8-mer helix will eventually collapse into the lower-energy globular form, but the kinetics of the process must be taken into account. For the 4-mer and 6-mer duplexes (assuming they were helical in solution), this transformation to the globular form must be very fast and occur before the ions reach the drift cell because no helical structures are observed in the ATDs. As the oligonucleotide increases in length, this transformation is expected to take longer. Molecular dynamics simulations at 300 K show this trend as they indicate that the 4-mer duplexes collapse into its globular form after 250 ps, the 6-mer duplexes collapse after 1500 ps, and the 8-mer duplexes retain a helical motif for at least 2000 ps. According to the ATD results, the 8-mer helical structures must have gas-phase lifetimes on the order of 1 millisecond (the time scale of the experiment) before they collapse into the globular form.

10-mer, 14-mer, and 18-mer Duplexes. The ATDs for the 10-mer, 14-mer, and 18-mer duplexes show only one peak, and the cross sections extracted from the ATDs are quite large (see Table 1). In the modeling, the starting geometries for the duplexes were helical, but the structures collapsed into lower-energy, globular forms during the simulated annealing process. Examples of the lowest energy structures for the 10-mer [duplex − 5H]$^{5-}$, 14-mer [duplex − 7H]$^{7-}$, and 18-mer [duplex − 9H]$^{9-}$ are shown in Figures 8a, 9a, and 10a. In each case, 3−5 Watson−Crick pairs remain intact, but the structure has lost any sense of helicity. However, the average cross sections of these globular forms are 10−15% smaller than experimental values.

The ATDs for the 8-mer duplex indicate that both globular and helical-like structures were present in the gas phase. The single peaks in the ATDs of the 10-mer, 14-mer, and 18-mer correlate with the peak assigned as helical in the 8-mer, and it is not unreasonable that a helical structure becomes more stable as strand length increases.
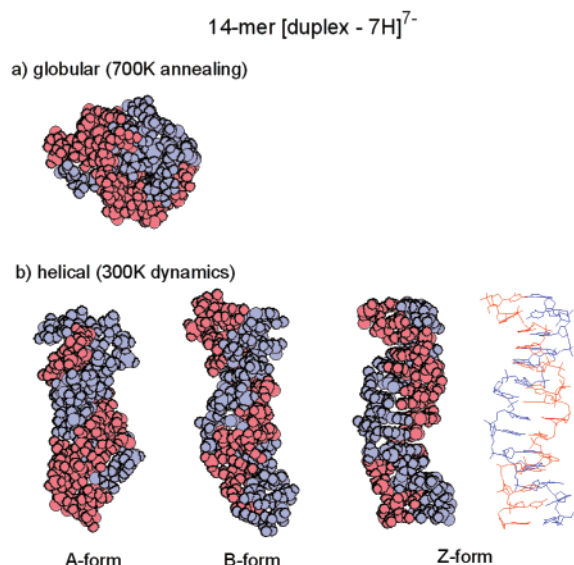
Figure 9. Space-filling models of the 14-mer [duplex − 7H]$^{7-}$ ion. (a) Lowest energy globular structure generated by the 700 K simulated annealing procedure. (b) Final structures after 5 ns of 300 K dynamics when starting with A-, B-, and Z-helices. A wire frame model of the Z-form is also shown to illustrate the retention of Watson−Crick pairing in the dynamics.
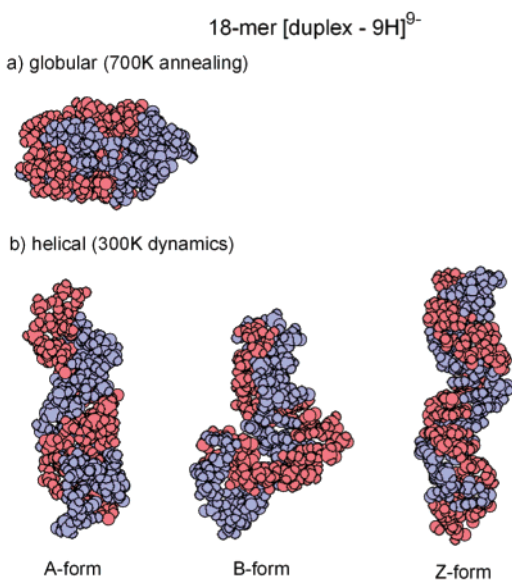

Figure 10. Space-filling models of the 18-mer [duplex − 9H]$^{9-}$ ion. (a) Lowest energy globular structure generated by the 700 K simulated annealing procedure. (b) Final structures after 5 ns of 300 K dynamics when starting with A-, B-, and Z-helices.

Plots of cross section versus dynamics time for the 10-mer, 14-mer, and 18-mer duplexes at 300 K are similar to those shown in Figure 7 for the 8-mer duplex. That is, the cross sections of the initial A- and B-forms rapidly decrease at the beginning of the dynamics but then level out over the final 1500 ps. The cross sections of the initial Z-forms do not decrease as much, and the final structures at the end of the dynamics are similar to the original starting structures. The final A-, B-, and Z-forms obtained at the end of the dynamics are shown in Figures 8b (10-mer), 9b (14-mer), and 10b (18-mer). The calculated cross sections of each form (averaged over the final 50−75 structures) are listed in Table 1.

Table 2. Relative Energy Differences (kcal/mol) between the Helical (A-, B-, and Z-forms) and Globular Forms of the Poly d(CG)$_n$ Duplexes

duplex	A-form	B-form	Z-form
[8mer + Na − 5H]$^{4-}$	130	110	110
[10mer − 5H]$^{5-}$	70	150	115
[14mer − 7H]$^{7-}$	50	130	90
[18mer − 9H]$^{9-}$	60	140	90

In the 10-mer duplex, 9 of 10 Watson−Crick pairs are retained in the A- and B-forms, and all 10 Watson−Crick pairs are retained in the Z-form. The final structures at the end of the dynamics simulations are distorted versions of their starting helical structures, but are definitely not globular. The B-form distorted the most during the dynamics simulation and yielded a final structure with the largest cross section (9% larger than experiment). The main disruptions in the B-helix arise from changes in base stacking within each strand. The bases remain stacked during the dynamics run, but they are not all perpendicular to the helical axis as they are in the original B-form, in some instances stacking in a T-shaped arrangement. Thus, the final B-form does not turn in the same manner as the starting B-helix. The Z-form distorted the least during the dynamics (in terms of changes in base stacking), but the final Z-helix still has a cross section that is 5% larger than experiment. The A-form, however, does yield a final structure whose cross section agrees well (2%) with experiment. The bases in the A-form at the end of the dynamics run are not all perpendicular to the helical axis, but the differences are not as great as in the B-form.

In the 14-mer duplexes, 12 of 14 Watson−Crick pairs are retained in the A- and B-forms, and all 14 Watson−Crick pairs are retained in the Z-form. Base stacking also appears to be better conserved given that the final helices are not as distorted from their original starting geometries as in the 8- and 10-mer duplexes. The average cross section of the 14-mer A-form agrees best with the experimental value (<1.5%), similar to the results obtained for the 8-mer and 10-mer duplexes, whereas the cross sections of the B- and Z-forms are ~3.5% larger than experiment. Molecular dynamics calculations also indicate that the A-form is the most stable helix in the gas phase. Helical structures are higher in energy than the globular forms for all of the duplexes, but as the length of the duplex increases, the magnitude of the energy difference tends to decrease, especially for the A-form. Table 2 shows this trend.

In the 18-mer duplex, all Watson−Crick pairs are retained in the A- and Z-forms, and only one Watson−Crick pair is broken in the B-form. The resulting helices at the end of the dynamics simulations appear very similar to the starting helices for the A- and Z-forms, but the B-form is vastly different. The bases in the B-form remain stacked during the dynamics run, but the whole helix bends, yielding a final structure with a cross section 4% smaller than the experiment cross section. The Z-form also bends, but only slightly, which causes a cross section that again is smaller than the experimental value. For the first time, the A-form helix resulting at the end of the dynamics simulations is larger than the B- and Z-forms (Table 1). This occurs because the A-form does not bend and instead looks very similar to its starting structure where the bases are perpendicular to the helical axis. The average cross section of the 18-mer A-form correlates best with the experimental value

(~1%), and it is the most energetically stable helix in the gas phase, similar to the 10-mer and 14-mer A-forms (Table 2).

Even though the globular forms are the energetically favored conformers in the gas phase, only helical conformers are observed in the ATDs for the 10-mer, 14-mer, and 18-mer duplexes. Thus, the larger duplexes must originally be helical in solution and retain a similar shape when the solvent evaporates, at least over the experimental time scale (~1 ms). The CD results on the 14-mer duplex (Figure 3) indicated that it is a B-DNA helix in solution, but comparison of theoretical and experimental cross sections and relative energy differences indicate that it most likely resembles a distorted A-helix in the gas phase. Previous data on DNA duplexes have shown that a B-form will convert to an A-form at low humidity or when the solution is changed to more apolar solvents.[53–55] Therefore, it is not unreasonable to presume that the duplexes can change from B-forms to A-forms during the desolvation process that occurs in the ESI event. As the ions travel from the source to the drift cell, the duplex distorts from a true A-helix but does not yet convert into the lower-energy globular form before it reaches the detector.

(53) Saenger, W. *Principles of Nucleic Acid Structure*; Springer-Verlag: New York, 1984.
(54) Franklin, R. E.; Gosling, R. G. *Acta Crystallogr.* **1953**, *6*, 673.
(55) Ivanov, V. I.; Krylov, D. Y. *Methods Enzymol.* **1992**, *211*, 111.

Conclusion

In summary, a growing number of ESI-MS studies have demonstrated that DNA duplexes can be transferred intact from solution to the gas phase. The ion mobility and molecular dynamics results presented here for a series of [poly d(CG)$_n$·poly d(CG)$_n$] duplexes indicate that not only are duplexes stable in the gas phase, but they can retain helical structures in solvent-free environments. For the 4-mer and 6-mer duplexes, only globular structures are observed. When the duplex reaches the 8-mer length, the globular form is the dominant conformer, but a small fraction of helical structures are also observed. For the 10-mer, 14-mer, and 18-mer duplexes, only helical structures are observed in the ion mobility experiments. Molecular dynamics calculations indicate that globular forms are the energetically favorable conformer for the duplexes in the gas phase, but the relative stability of helical structures increases as the length of the duplex strands increases. Thus, the longer duplexes must have been helical in solution and retain that conformation for a limited time in the gas phase.

JA046433+